Editors' Suggestion

Absence of a bulk thermodynamic phase transition to a density wave phase in UTe_2

Florian Theuss,[1] Avi Shragai,[1] Gael Grissonnanche,[1,2,3] Luciano Peralta,[4] Gregorio de la Fuente Simarro,[1] Ian M Hayes,[5] Shanta R Saha,[5] Yun Suk Eo,[5] Alonso Suarez,[5] Andrea Capa Salinas,[6] Ganesh Pokharel,[6] Stephen D. Wilson,[6] Nicholas P Butch,[5,7] Johnpierre Paglione,[5,8] and B. J. Ramshaw[1,8,*]

[1]*Laboratory of Atomic and Solid State Physics, Cornell University, Ithaca, New York 14853, USA*
[2]*Kavli Institute at Cornell for Nanoscale Science, Ithaca, New York 14853, USA*
[3]*Laboratoire des Solides Irradiés, CEA/DRF/lRAMIS, CNRS, École Polytechnique, Institut Polytechnique de Paris, F-91128 Palaiseau, France*
[4]*Department of Physics, Universidad de Los Andes, Bogota 111711, Colombia*
[5]*Maryland Quantum Materials Center, Department of Physics, University of Maryland, College Park, Maryland 20742, USA*
[6]*Materials Department, University of California Santa Barbara, Santa Barbara, California 93106, USA*
[7]*NIST Center for Neutron Research, National Institute of Standards and Technology, 100 Bureau Drive, Gaithersburg, Maryland 20899, USA*
[8]*Canadian Institute for Advanced Research, Toronto, Ontario, Canada, M5G 1M1*

(Received 9 July 2024; revised 11 September 2024; accepted 16 September 2024; published 9 October 2024)

Competing and intertwined orders are ubiquitous in strongly correlated electron systems, such as the charge, spin, and superconducting orders in the high-T_c cuprates. Recent scanning tunneling microscopy (STM) measurements provide evidence for a charge density wave (CDW) that coexists with superconductivity in the heavy fermion metal UTe_2. This CDW persists up to at least 7.5 K, and, as a CDW breaks the translational symmetry of the lattice, its disappearance is necessarily accompanied by a thermodynamic phase transition. We report high-precision thermodynamic measurements of the elastic moduli of UTe_2. We observe no signature of a phase transition in the elastic moduli down to a level of 1 part in 10^7, strongly implying the absence of bulk CDW order in UTe_2. We suggest that the CDW and associated pair density wave observed by STM may be confined to the surface of UTe_2.

DOI: 10.1103/PhysRevB.110.144507

I. INTRODUCTION

The superconductivity of UTe_2 is unconventional in many respects: it is spin triplet [1], it has a reentrant phase at very high magnetic fields [2,3], and its superconducting T_c bifurcates into two transitions under pressure [4,5]. Recent scanning tunneling microscopy (STM) experiments [6–9] have provided evidence for even more unusual behavior: the coexistence of superconductivity with an incommensurate charge density wave (CDW). Upon applying a magnetic field, superconductivity and the CDW are suppressed at the same critical field [6]. This observation suggests a close connection between superconductivity and the CDW in UTe_2, potentially connected via a parent pair density wave (PDW) [8].

STM measurements clearly indicate that the CDW persists up to at least 7.5 K—more than a factor of 3 higher than T_c—and disappears at a temperature no higher than 12 K [9]. A corollary of this observation is that, upon cooling below 12 K, UTe_2 first enters a broken-symmetry CDW phase, followed by the onset of superconductivity at lower temperature. As broken-symmetry phases are necessarily accompanied by thermodynamic phase transitions [10], it is natural to ask whether such a phase transition is observed between 7.5 and 12 K in UTe_2. The answer thus far is negative: the superconducting transition is the only phase transition visible in specific-heat measurements at ambient pressures and in zero magnetic field [11].

The apparent absence of a second phase transition leads to the following question: does CDW order exist in the bulk of UTe_2, or is it confined to the surface? This gets to the heart of a broader problem: which of the many exotic phenomena that have been discovered in UTe_2 are representative of the bulk, and which are particular to the surface? For example, the polar Kerr effect [12], STM [13], and microwave conductivity [14] measurements all suggest a two-component, time-reversal symmetry-breaking order parameter, whereas ultrasound [15] and some specific-heat [16] measurements suggest a single-component order parameter. One possible resolution is that Kerr, STM, and microwaves are all sensitive to a unique superconducting state on the surface of UTe_2, whereas ultrasound and specific heat are sensitive to the bulk order parameter. This issue of bulk versus surface superconductivity in UTe_2 is closely related to the existence of a CDW, as a superconducting PDW is necessarily accompanied by a CDW. The existence of such a PDW/CDW pair in the bulk would strongly constrain the microscopic mechanism of Cooper pairing in UTe_2. To investigate the possibility of a phase transition to bulk CDW order in UTe_2, we measure the elastic moduli as a function of temperature, from 2 to 280 K. Elastic moduli

*Contact author: bradramshaw@cornell.edu

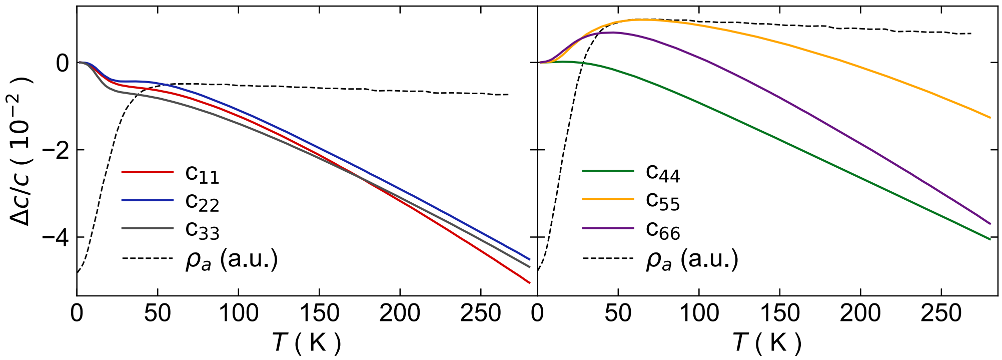

FIG. 1. Elastic moduli of UTe_2 from 2 to 280 K. The three compressional moduli (left) and shear moduli (right) are shown from 1.2 to 300 K. $\Delta c/c$ is defined as $[c(T) - c(2\,\mathrm{K})]/c(2\,\mathrm{K})$. The *a*-axis resistivity of UTe_2 is plotted as a dashed line for comparison and is taken from Eo *et al.* [17]. The downturn of the resistivity around 50 K coincides with deviations from conventional stiffening due to lattice anharmonicity in c_{11}, c_{22}, c_{33}, c_{55}, and c_{66}. Note that the noise in the data is smaller than the width of the lines on this scale.

are particularly sensitive to CDW phase transitions because they break the translational symmetry of the lattice. This has been investigated extensively in other CDW systems, such as the rare-earth tritellurides, where discontinuities in the elastic moduli at T_{CDW} are of order a few times 10^{-2} of the total elastic moduli [18]. Because elastic moduli can be measured with better than one part in 10^7 precision (see the Methods section), our measurements have many decades of sensitivity to explore the possibility of a bulk phase transition to CDW order in UTe_2.

II. RESULTS

Elastic moduli, c_{ij}, are the thermodynamic coefficients characterizing the susceptibility of a material to strain. In terms of the total free energy $\mathcal{F}$, elastic moduli are given by

$$c_{ij} = \frac{\partial^2 \mathcal{F}}{\partial \epsilon_{ij}^2}, \tag{1}$$

where ϵ_{ij} is a particular component of the strain tensor. These moduli are related to the sound velocities, v_{ij}, by $v_{ij} = \sqrt{c_{ij}/\rho}$, where ρ is the material density. Like other thermodynamic susceptibilities, such as specific heat, elastic moduli exhibit singular behavior at phase transitions [19].

We first show the elastic moduli corresponding to all six unique strains in UTe_2 measured over a broad temperature range—from 2 to 280 K—using pulse echo ultrasound. These data are reproduced from Theuss *et al.* [15], where details about the sample preparation and experimental technique are given.

All six elastic moduli exhibit only smooth behavior across the entire temperature range down to T_c. The shear modulus c_{44} exhibits conventional stiffening due to lattice anharmonicity [20]. The other two shear (c_{55} and c_{66}) and three compressional moduli (c_{11}, c_{22}, and c_{33}) exhibit smooth evolution with temperature that is associated with the onset of Kondo coherence near 50 K [21,22]. This demonstrates the sensitivity of five out of six elastic moduli to changes in the electronic structure of UTe_2. Despite this sensitivity, no sharp changes in slope or discontinuities that would be indicative of an electronic phase transition are visible on this scale.

To further constrain the presence or absence of a CDW transition, we performed high-resolution resonant ultrasound spectroscopy (RUS) measurements on UTe_2 across the temperature range where the CDW peaks disappear in the STM experiments [9]. RUS measures the mechanical resonance frequencies of a sample. Each resonance frequency is determined by the sample geometry, the material density, and the elastic moduli. While procedures exist for decomposing the temperature dependence of the resonance frequencies into the temperature dependence of the elastic moduli [23–25] (see Methods), the highest signal to noise is obtained by directly examining the resonance frequencies.

Figure 2 shows the temperature dependence of five resonance frequencies from 4 to 20 K—across the temperature range where the CDW disappears in the STM experiments. No anomalies are visible across the entire temperature range. These resonance frequencies contain admixtures of all nine elastic moduli in different proportions: the topmost resonance (blue) is dominated by compressional moduli, whereas the resonance at the bottom of the figure (green) is dominated by shear moduli. Thus, all resonances should show a singular jump, as well as a change in slope, at a phase transition [26]. Using the signal-to-noise of our measurement, we can constrain any singularity in the elastic moduli to be smaller than 1×10^{-7} (see Methods).

To provide a sense of scale for what is expected at a CDW transition, we perform similar RUS measurements on CsV_3Sb_5. CsV_3Sb_5 has both a CDW transition near 90 K and a superconducting T_c near 2 K [27]. The analogy with UTe_2 is close, as there is also STM evidence for a PDW in this material [28]. The impact of the CDW phase transition on the elastic moduli is striking: discontinuities on the order of 2×10^{-2} are visible at T_{CDW}—five orders of magnitude larger than our signal to noise in UTe_2. Similar-sized anomalies at T_{CDW} are present in the elastic moduli of the rare-earth tritellurides, and anomalies of order 10^{-4} are found at the transition to the

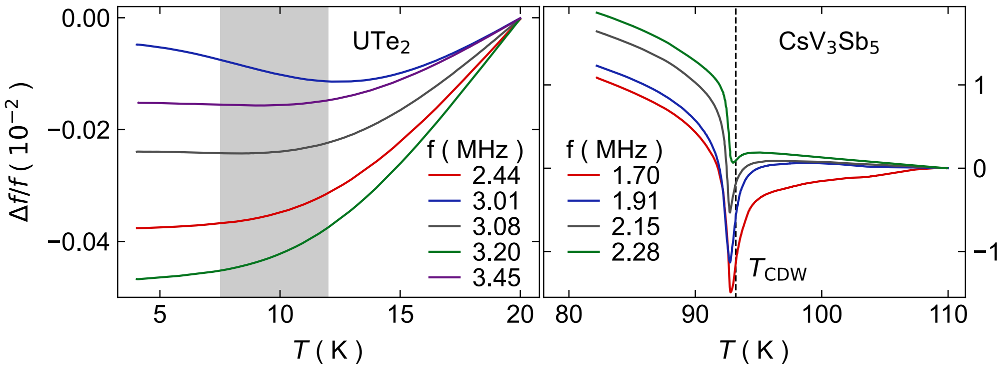

FIG. 2. Low-temperature elastic resonances of CsV_3Sb_5 and UTe_2. High-resolution mechanical resonances of UTe_2 (left) and CsV_3Sb_5 (right). Each curve tracks the frequency of a single mechanical resonance of a single-crystal sample. $\Delta f/f$ is defined as $[f(T) - f(T_0)]/f(T_0)$, where T_0 is the highest temperature shown. A gray bar indicates the temperature range over which the CDW disappears in STM measurements of UTe_2. Note that the noise in the data is smaller than the width of the lines on this scale.

high-field CDW phase of the high-T_c cuprates. These results are summarized, along with other examples from the literature, in Table I.

III. DISCUSSION

Our data constrain any thermodynamic signature of a CDW phase transition in UTe_2 to be $\Delta c/c < 1 \times 10^{-7}$. This is five orders of magnitude smaller than what is observed in CsV_3Sb_5 and in the rare-earth tritellurides [18], and three orders of magnitude smaller than what is observed in the high-T_c cuprates. This constraint is two orders of magnitude tighter than that placed by previous thermal expansion [11,29] and specific-heat [30] measurements on UTe_2 (these investigations did not discuss the absence of a CDW transition, but they do present data taken over the relevant temperature range).

There are two common arguments as to why a CDW might not exhibit a thermodynamic signature in the elastic moduli: from broadening of the transition due to disorder, and from insensitivity of the CDW to the lattice (a "purely electronic" CDW). We address these possibilities in turn.

Disorder tends to broaden all thermodynamic singularities at a CDW transition [31,32]. This is most apparent in the high-T_c cuprates. There, CDW correlation lengths range from a few unit cells in $Bi_2Sr_2CaCu_2O_{8+\delta}$ [34] to roughly 100 Å in $YBa_2Cu_3O_{6+\delta}$ [35–37]. Because of the short correlation length, no anomaly is found in either the specific heat or the elastic moduli at the onset of the CDW correlations [38,39]. Only upon applying a magnetic field is the correlation length increased to roughly 300 Å and an associated singularity observed in the elastic moduli [38,40]. The CDW seen by STM in UTe_2 is qualitatively different from that found in the cuprates: in UTe_2, the CDW peaks are of a similar width to the crystalline Bragg peaks [6]. Furthermore, existing ultrasound investigations into the superconducting state of UTe_2 reveal sharp superconducting transitions—with widths only 5% of T_c—that show no signs of broadening due to disorder [15]. Thus disorder is an unlikely explanation for the lack of thermodynamic singularity at a putative T_{CDW}.

A "purely electronic" CDW would be a CDW that is entirely decoupled from the crystalline lattice. To our knowledge, such a state does not exist. The very fact that UTe_2 has a non-Galilean-invariant (i.e., nonspherical) Fermi surface [41] means that the electronic degrees of freedom are coupled to the lattice potential. As sound waves deform that lattice potential, they are necessarily coupled to the conduction electrons.

TABLE I. Elastic moduli discontinuities in several CDW materials. $Y_{[ijk]}$ is a Young's modulus measured with the compressive stress in the [ijk] direction. $NbSe_2$, CsV_3Sb_5, $YBa_2Cu_3O_{6.55}$, and $Lu_5Ir_4Si_{10}$ also have superconducting transitions at lower temperatures. The elastic anomaly in $TbTe_3$ is representative of all rare-earth tritellurides [33].

Material	T_{CDW}(K)	$\Delta c/c$	c_{ij}	Reference
UTe_2	10 − 12	$<1 \times 10^{-7}$		This work
CsV_3Sb_5	93	$\approx 10^{-2}$		This work
$TbTe_3$	333	2×10^{-2}	c_{11}	Saint-Paul *et al.* [18]
		2×10^{-2}	c_{33}	
$K_{0.3}MoO_3$	180	2×10^{-2}	$Y_{[102]}$	Brill *et al.* [42]
$Lu_5Ir_4Si_{10}$	80	1×10^{-2}	c_{11}	Saint-Paul *et al.* [43]
		6×10^{-3}	c_{33}	
TTF-TCNQ	53	1×10^{-2}	$Y_{[010]}$	Barmatz *et al.* [44]
2*H*-$NbSe_2$	30	1×10^{-3}	$Y_{[100]}$	Barmatz *et al.* [45]
$YBa_2Cu_3O_{6.55}$ ($H = 30$ T)	50	8×10^{-5}	c_{22}	Laliberté *et al.* [38]

TABLE II. Resonance frequency composition. The coefficient of each elastic modulus that makes up the resonance frequency as defined in Eq. (2).

f (MHz)	α_{11}	α_{22}	α_{33}	α_{12}	α_{13}	α_{23}	α_{44}	α_{55}	α_{66}
2.44	0.141	0.088	0.212	0.004	−0.092	−0.028	0.263	0.129	0.283
3.01	0.250	0.178	0.310	−0.022	−0.152	−0.045	0.190	0.168	0.123
3.08	0.241	0.113	0.190	−0.030	−0.115	−0.007	0.233	0.129	0.246
3.20	0.191	0.082	0.244	−0.004	−0.134	−0.020	0.246	0.146	0.249
3.45	0.212	0.108	0.190	−0.015	−0.109	−0.018	0.248	0.110	0.274

This is evidenced by softening of the elastic moduli at the onset of Kondo coherence near 50 K (Fig. 1), as well as by the sharp thermodynamic singularities seen at T_c [15]. Any redistribution of the charge density in a metal is necessarily compensated for by a displacement of the lattice to maintain local charge neutrality, and thus a thermodynamic signature in the elastic moduli at a CDW transition is inescapable.

We find no evidence for a transition to a CDW phase in the bulk of UTe_2, despite such evidence existing on the [011] surface as measured by STM [6–9]. Indeed, there are other examples of CDWs that exist only on the surfaces of metals [46–48]. Our observation is also consistent with the lack of a CDW phase transition occurring in other bulk-sensitive probes such as heat capacity [30], thermal expansion [11,29], and NMR [49]. We also note that recent x-ray diffraction measurements have failed to detect the requisite superlattice peaks expected for a CDW [50]. This suggests that the surface of UTe_2 may host different ordered states from the bulk, including possibly a different superconducting order parameter. Thus, while the host of unconventional phenomena discovered by both bulk and surface measurements in UTe_2 must ultimately be understood within a single framework, one should be careful when extrapolating observations made on the surface to the bulk and vice versa.

IV. METHODS

A. Sample preparation

1. CsV_3Sb_5

Single crystals of CsV_3Sb_5 were synthesized by the self-flux method in an inert environment. Elemental liquid Cs (Alfa 99.98%), V powder (Sigma 99.9%) in-house prepurified in a 9:1 ethanol/hydrochloric acid mixture, and Sb shot (Alfa 99.999%) were weighed out to $Cs_{20}V_{15}Sb_{120}$ stoichiometry and milled in a tungsten carbide vial. The precursor milled powder was heated up to 1000 °C, soaked for 12 h, cooled down to 900 °C at 5 °C/h, and further cooled down to 500 °C at 2 °C. Once at room temperature, the resulting crystals were extracted manually in air.

A single-crystal specimen was selected for RUS based on visual inspection. Samples with cracks, excessive flux, and intergrowth of secondary phases were avoided due to their detrimental effects on the mechanical quality factors. The sample chosen for the RUS measurements presented here is irregularly shaped, with two parallel faces perpendicular to the crystallographic c axis. Its dimensions are roughly 0.5×0.8 mm^2 in the a-b plane and 0.09 mm along the c axis.

2. UTe_2

Single crystals of UTe_2 were grown by the chemical vapor transport method as described in Ran *et al.* [51].

The sample used for the RUS measurement was a roughly $1 \times 1 \times 1$ mm^3 large, irregularly shaped sample. More details on the shape of this sample are found in Theuss *et al.* [24] under Sample B.

The surface of a single-crystal specimen was digitized using a Zeiss Xradia Versa XRM-520 X-ray nano-CT, and the digitized mesh was aligned to the crystal axes using back-reflection Laue.

B. Experiments

1. Pulse-echo ultrasound

Measurements were performed in an Oxford Instruments Heliox ^{3}He refrigerator using a traditional phase-comparison pulse-echo method. Measurements were performed on three different samples in six different transducer configurations. More details about the samples and experiment can be found in the Methods section of Theuss *et al.* [15].

2. Resonant ultrasound spectroscopy

We performed RUS on a single-crystal sample of UTe_2 in a custom-built probe immersed in a bath of ^{4}He. Details of the apparatus and the procedure for measuring resonance frequencies can be found in the Methods section of Ghosh *et al.* [52]. Temperature sweeps were performed using a slow ramp rate of approximately 0.025 K/min.

We fit the elastic moduli of this sample at 4 K using the method described in Theuss *et al.* [24]. The absolute elastic moduli for this sample are found in Table III of Theuss *et al.* [24] under Sample B. The raw resonance frequencies, as well as the fit we obtain, are found in Table XI of the supplemental material to Theuss *et al.* [24].

The fit to the resonance spectrum allows us to determine the contribution from each elastic modulus to each resonance frequency. Each resonance frequency f_k contains contributions from all elastic moduli, and the relative change in resonance frequency as a function of temperature is given by

$$\frac{\Delta f_k}{f_k} = \sum_{i,j} \alpha_{ij}^{(k)} \frac{\Delta c_{ij}}{c_{ij}}, \tag{2}$$

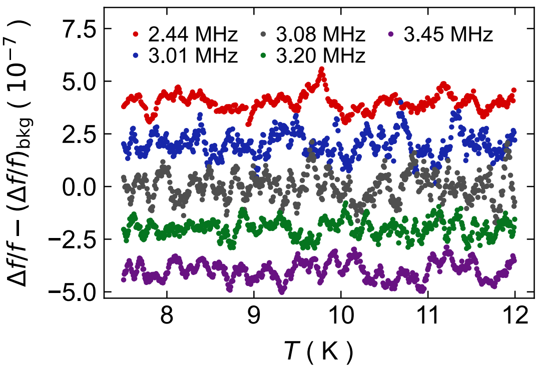

FIG. 3. Noise level of UTe_2 resonances. The same data as presented in Fig. 2 but with a fifth-order polynomial background subtracted. The spacing between points is approximately 8 mK, and the data have had a moving average applied over a 10-point window. The data have been offset vertically for clarity.

where the $\alpha_{ij}^{(k)}$ coefficients are temperature-independent, $\Delta f_k/f_k \equiv [f_k(T) - f_k(T_0)]/f_k(T_0)$ is the relative change in resonance frequency referenced to temperature T_0, and likewise for $\Delta c_{ij}/c_{ij}$. The coefficients $\alpha_{ij}^{(k)}$ sum to 1 for each resonance: $\sum_{i,j} \alpha_{ij}^{(k)} = 1$.

Figure 2 shows five resonance frequencies selected for having high Q factors ($>10^5$) and qualitatively different temperature dependencies such that all elastic moduli are represented in this data set. This representation is quantified through the $\alpha_{ij}^{(k)}$ coefficients of Eq. (2). Table II shows these coefficients for the five resonance frequencies plotted in Fig. 2.

Discontinuities are expected in the three compressional elastic moduli—c_{11}, c_{22}, and c_{33}—at any phase transition [52], irrespective of which symmetries are broken (shear moduli can have discontinuities for some, but not all order parameters). Thus, it is critical that the three compressional moduli are well-represented in the resonance frequencies we analyze. Table II shows that the temperature dependences of c_{11}, c_{22}, and c_{33} each make up between 10% and 30% of the total frequency shift for the five resonances shown in Fig. 2. Thus if there was a phase transition, these five frequencies would show it.

C. Noise analysis

Figure 3 shows the same UTe_2 RUS data from Fig. 2, but with a fifth-order polynomial subtracted and a moving average of 10 points applied. With a temperature step of approximately 8 mK, this averages over an 80 mK window—the same width as the thermodynamic singularity at T_c in UTe_2 [15]. The noise on this scale is of order $\Delta f/f \approx \pm 1 \times 10^{-7}$.

ACKNOWLEDGMENTS

A.S., B.J.R., and F.T. acknowledge funding from the U.S. Department of Energy Office of Basic Energy Sciences under Award No. DE-SC0020143 (ultrasound experiments and analysis). N.B. and J.P. acknowledge support from the Department of Energy Award No. DE-SC-0019154 (sample characterization), the Gordon and Betty Moore Foundation's EPiQS Initiative through Grant No. GBMF9071 (materials synthesis), the National Science Foundation under Grant No. DMR-2105191 (sample preparation), and the Maryland Quantum Materials Center and the National Institute of Standards and Technology. B.J.R. and F.T. acknowledge use of the Cornell Center for Materials Research Shared Facilities, which are supported through the NSF MRSEC program (DMR-1719875).

[1] G. Nakamine, S. Kitagawa, K. Ishida, Y. Tokunaga, H. Sakai, S. Kambe, A. Nakamura, Y. Shimizu, Y. Homma, D. Li *et al.*, Superconducting properties of heavy Fermion UTe_2 revealed by ^{125}Te-nuclear magnetic resonance, J. Phys. Soc. Jpn. **88**, 113703 (2019).

[2] S. Ran, C. Eckberg, Q.-P. Ding, Y. Furukawa, T. Metz, S. R. Saha, I.-L. Liu, M. Zic, H. Kim, J. Paglione *et al.*, Nearly ferromagnetic spin-triplet superconductivity, Science **365**, 684 (2019).

[3] S. Ran, I.-L. Liu, Y. S. Eo, D. J. Campbell, P. M. Neves, W. T. Fuhrman, S. R. Saha, C. Eckberg, H. Kim, D. Graf, F. Balakirev, J. Singleton, J. Paglione, and N. P. Butch, Extreme magnetic field-boosted superconductivity, Nat. Phys. **15**, 1250 (2019).

[4] D. Aoki, F. Honda, G. Knebel, D. Braithwaite, A. Nakamura, D. X. Li, Y. Homma, Y. Shimizu, Y. J. Sato, J. P. Brison, and J. Flouquet, Multiple superconducting phases and unusual enhancement of the upper critical field in UTe_2, J. Phys. Soc. Jpn. **89**, 053705 (2020).

[5] D. Braithwaite, M. Vališka, G. Knebel, G. Lapertot, J.-P. Brison, A. Pourret, M. E. Zhitomirsky, J. Flouquet, F. Honda, and D. Aoki, Multiple superconducting phases in a nearly ferromagnetic system, Commun. Phys. **2**, 147 (2019).

[6] A. Aishwarya, J. May-Mann, A. Raghavan, L. Nie, M. Romanelli, S. Ran, S. R. Saha, J. Paglione, N. P. Butch, E. Fradkin, and V. Madhavan, Magnetic-field-sensitive charge density waves in the superconductor UTe_2, Nature (London) **618**, 928 (2023).

[7] A. Aishwarya, J. May-Mann, A. Almoalem, S. Ran, S. R. Saha, J. Paglione, N. P. Butch, E. Fradkin, and V. Madhavan, Melting of the charge density wave by generation of pairs of topological defects in UTe_2, Nat. Phys. **20**, 964 (2024).

[8] Q. Gu, J. P. Carroll, S. Wang, S. Ran, C. Broyles, H. Siddiquee, N. P. Butch, S. R. Saha, J. Paglione, J. C. S. Davis, and X. Liu, Detection of a pair density wave state in UTe_2, Nature (London) **618**, 921 (2023).

[9] A. LaFleur, H. Li, C. E. Frank, M. Xu, S. Cheng, Z. Wang, N. P. Butch, and I. Zeljkovic, Inhomogeneous high temperature melting and decoupling of charge density waves in spin-triplet superconductor UTe_2, Nat. Commun. **15**, 4456 (2024).

[10] L. D. Landau, On the theory of phase transitions, Zh. Eksp. Teor. Fiz. **7**, 19 (1937).

[11] K. Willa, F. Hardy, D. Aoki, D. Li, P. Wiecki, G. Lapertot, and C. Meingast, Thermodynamic signatures of short-range magnetic correlations in UTe_2, Phys. Rev. B **104**, 205107 (2021).

[12] I. M. Hayes, D. S. Wei, T. Metz, J. Zhang, Y. S. Eo, S. Ran, S. R. Saha, J. Collini, N. P. Butch, D. F. Agterberg *et al.*, Multicomponent superconducting order parameter in UTe_2, Science **373**, 797 (2021).

[13] L. Jiao, S. Howard, S. Ran, Z. Wang, J. O. Rodriguez, M. Sigrist, Z. Wang, N. P. Butch, and V. Madhavan, Chiral superconductivity in heavy-fermion metal UTe_2, Nature (London) **579**, 523 (2020).

[14] S. Bae, H. Kim, Y. S. Eo, S. Ran, I.-l. Liu, W. T. Fuhrman, J. Paglione, N. P. Butch, and S. M. Anlage, Anomalous normal fluid response in a chiral superconductor UTe_2, Nat. Commun. **12**, 2644 (2021).

[15] F. Theuss, A. Shragai, G. Grissonnanche, I. M. Hayes, S. R. Saha, Y. S. Eo, A. Suarez, T. Shishidou, N. P. Butch, J. Paglione *et al.*, Single-component superconductivity in UTe_2 at ambient pressure, Nat. Phys. **20**, 1124 (2024).

[16] P. F. S. Rosa, A. Weiland, S. S. Fender, B. L. Scott, F. Ronning, J. D. Thompson, E. D. Bauer, and S. M. Thomas, Single thermodynamic transition at 2 K in superconducting UTe_2 single crystals, Commun. Mater. **3**, 33 (2022).

[17] Y. S. Eo, S. Liu, S. R. Saha, H. Kim, S. Ran, J. A. Horn, H. Hodovanets, J. Collini, T. Metz, W. T. Fuhrman, A. H. Nevidomskyy, J. D. Denlinger, N. P. Butch, M. S. Fuhrer, L. A. Wray, and J. Paglione, *c*-axis transport in UTe_2: Evidence of three-dimensional conductivity component, Phys. Rev. B **106**, L060505 (2022).

[18] M. Saint-Paul, C. Guttin, P. Lejay, G. Remenyi, O. Leynaud, and P. Monceau, Elastic anomalies at the charge density wave transition in $TbTe_3$, Solid State Commun. **233**, 24 (2016).

[19] L. D. Landau and E. M. Lifshitz, *Statistical Physics* (Elsevier, Amsterdam, 2013), Vol. 5.

[20] Y. P. Varshni, Temperature dependence of the elastic constants, Phys. Rev. B **2**, 3952 (1970).

[21] B. Lüthi, Magnetoacoustics in intermetallic f-electron systems, J. Magn. Magn. Mater. **52**, 70 (1985).

[22] B. Löthi, G. Bruls, P. Thalmeier, B. Wolf, D. Finsterbusch, and I. Kouroudis, Electron-phonon effects in heavy fermion systems, J. Low Temp. Phys. **95**, 257 (1994).

[23] B. J. Ramshaw, A. Shekhter, R. D. McDonald, J. B. Betts, J. N. Mitchell, P. H. Tobash, C. H. Mielke, E. D. Bauer, and A. Migliori, Avoided valence transition in a plutonium superconductor, Proc. Natl. Acad. Sci. USA **112**, 3285 (2015).

[24] F. Theuss, G. de la F. Simarro, A. Shragai, G. Grissonnanche, I. M. Hayes, S. Saha, T. Shishidou, T. Chen, S. Nakatsuji, S. Ran *et al.*, Resonant ultrasound spectroscopy for irregularly shaped samples and its application to uranium ditelluride, Phys. Rev. Lett. **132**, 066003 (2024).

[25] W. M. Visscher, A. Migliori, T. M. Bell, and R. A. Reinert, On the normal modes of free vibration of inhomogeneous and anisotropic elastic objects, J. Acoust. Soc. Am. **90**, 2154 (1991).

[26] W. Rehwald, The study of structural phase transitions by means of ultrasonic experiments, Adv. Phys. **22**, 721 (1973).

[27] B. R. Ortiz, S. M. L. Teicher, Y. Hu, J. L. Zuo, P. M. Sarte, E. C. Schueller, A. M. M. Abeykoon, M. J. Krogstad, S. Rosenkranz, R. Osborn *et al.*, Cs V_3Sb_5: A $\mathbb{Z}_2$ topological kagome metal with a superconducting ground state, Phys. Rev. Lett. **125**, 247002 (2020).

[28] H. Chen, H. Yang, B. Hu, Z. Zhao, J. Yuan, Y. Xing, G. Qian, Z. Huang, G. Li, Y. Ye *et al.*, Roton pair density wave in a strong-coupling kagome superconductor, Nature (London) **599**, 222 (2021).

[29] S. M. Thomas, C. Stevens, F. B. Santos, S. S. Fender, E. D. Bauer, F. Ronning, J. D. Thompson, A. Huxley, and P. F. S. Rosa, Spatially inhomogeneous superconductivity in UTe_2, Phys. Rev. B **104**, 224501 (2021).

[30] Y. Haga, P. Opletal, Y. Tokiwa, E. Yamamoto, Y. Tokunaga, S. Kambe, and H. Sakai, Effect of uranium deficiency on normal and superconducting properties in unconventional superconductor UTe_2, J. Phys.: Condens. Matter **34**, 175601 (2022).

[31] R. F. Luccas, A. Fente, J. Hanko, A. Correa-Orellana, E. Herrera, E. Climent-Pascual, J. Azpeitia, T. Pérez-Castañeda, M. R. Osorio, E. Salas-Colera, N. M. Nemes, F. J. Mompean, M. García-Hernández, J. G. Rodrigo, M. A. Ramos, I. Guillamón, S. Vieira, and H. Suderow, Charge density wave in layered $La_{1-x}Ce_xSb_2$, Phys. Rev. B **92**, 235153 (2015).

[32] Y. Singh, R. Nirmala, S. Ramakrishnan, and S. K. Malik, Competition between superconductivity and charge-density-wave ordering in the $Lu_5Ir_4(Si_{1-x}Ge_x)_{10}$ alloy system, Phys. Rev. B **72**, 045106 (2005).

[33] M. Saint-Paul and P. Monceau, Phenomenological approach of the thermodynamic properties of the charge density wave systems, Philos. Mag. **101**, 598 (2021).

[34] J. E. Hoffman, E. W. Hudson, K. M. Lang, V. Madhavan, H. Eisaki, S. Uchida, and J. C. Davis, A four unit cell periodic pattern of quasi-particle states surrounding vortex cores in $Bi_2Sr_2CaCu_2O_{8+\delta}$, Science **295**, 466 (2002).

[35] S. Blanco-Canosa, A. Frano, E. Schierle, J. Porras, T. Loew, M. Minola, M. Bluschke, E. Weschke, B. Keimer, and M. Le Tacon, Resonant x-ray scattering study of charge-density wave correlations in $YBa_2Cu_3O_{6+x}$, Phys. Rev. B **90**, 054513 (2014).

[36] G. Ghiringhelli, M. Le Tacon, M. Minola, S. Blanco-Canosa, C. Mazzoli, N. B. Brookes, G. M. De Luca, A. Frano, D. G. Hawthorn, F. He *et al.*, Long-range incommensurate charge fluctuations in (Y, Nd) $Ba_2Cu_3O_{6+x}$, Science **337**, 821 (2012).

[37] T. Wu, H. Mayaffre, S. Krämer, M. Horvatić, C. Berthier, W. N. Hardy, R. Liang, D. A. Bonn, and M.-H. Julien, Magnetic-field-induced charge-stripe order in the high-temperature superconductor $YBa_2Cu_3O_y$, Nature (London) **477**, 191 (2011).

[38] F. Laliberté, M. Frachet, S. Benhabib, B. Borgnic, T. Loew, J. Porras, M. Le Tacon, B. Keimer, S. Wiedmann, C. Proust, and D. LeBoeuf, High field charge order across the phase diagram of $YBa_2Cu_3O_y$, npj Quantum Mater. **3**, 11 (2018).

[39] J. W. Loram, J. Luo, J. R. Cooper, W. Y. Liang, and J. L. Tallon, Evidence on the pseudogap and condensate from the electronic specific heat, J. Phys. Chem. Solids **62**, 59 (2001).

[40] S. Gerber, H. Jang, H. Nojiri, S. Matsuzawa, H. Yasumura, D. A. Bonn, R. Liang, W. N. Hardy, Z. Islam, A. Mehta *et al.*, Three-dimensional charge density wave order in $YBa_2Cu_3O_{6.67}$ at high magnetic fields, Science **350**, 949 (2015).

[41] D. Aoki, H. Sakai, P. Opletal, Y. Tokiwa, J. Ishizuka, Y. Yanase, H. Harima, A. Nakamura, D. Li, Y. Homma *et al.*, First observation of the de Haas–van Alphen effect and fermi surfaces in the unconventional superconductor UTe_2, J. Phys. Soc. Jpn. **91**, 083704 (2022).

[42] J. W. Brill, M. Chung, Y. K. Kuo, X. Zhan, E. Figueroa, and G. Mozurkewich, Thermodynamics of the charge-density-wave transition in blue bronze, Phys. Rev. Lett. **74**, 1182 (1995).

[43] M. Saint-Paul, C. Opagiste, and C. Guttin, Elastic anomalies at the first order transition in $Lu_5Ir_4Si_{10}$, J. Phys. Chem. Solids **138**, 109255 (2020).

[44] M. Barmatz, L. R. Testardi, A. F. Garito, and A. J. Heeger, Elastic properties of one dimensional compounds, Solid State Commun. **15**, 1299 (1974).

[45] M. Barmatz, L. R. Testardi, and F. J. Di Salvo, Elasticity measurements in the layered dichalcogenides $TaSe_2$ and $NbSe_2$, Phys. Rev. B **12**, 4367 (1975).

[46] T. Aruga, Charge-density waves on metal surfaces, J. Phys.: Condens. Matter **14**, 8393 (2002).

[47] J. J. Lander and J. Morrison, Structures of clean surfaces of germanium and silicon. I, J. Appl. Phys. **34**, 1403 (1963).

[48] P. T. Sprunger, L. Petersen, E. W. Plummer, E. Lægsgaard, and F. Besenbacher, Giant Friedel oscillations on the Beryllium(0001) surface, Science **275**, 1764 (1997).

[49] Y. Tokunaga, H. Sakai, S. Kambe, T. Hattori, N. Higa, G. Nakamine, S. Kitagawa, K. Ishida, A. Nakamura, Y. Shimizu, Y. Homma, D. Li, F. Honda, and D. Aoki, ^{125}Te-NMR study on a single crystal of heavy Fermion superconductor UTe_2, J. Phys. Soc. Jpn. **88**, 073701 (2019).

[50] C. S. Kengle, D. Chaudhuri, X. Guo, T. A. Johnson, S. Bettler, W. Simeth, M. J. Krogstad, Z. Islam, S. Ran, S. R. Saha *et al.*, companion paper, Absence of a bulk signature of a charge density wave in hard x-ray measurements of UTe_2, Phys. Rev. B **110**, 145101 (2024).

[51] S. Ran, I.-L. Liu, S. R. Saha, P. Saraf, J. Paglione, and N. P. Butch, Comparison of two different synthesis methods of single crystals of superconducting uranium ditelluride, J. Vis. Exp. **173**, e62563 (2021).

[52] S. Ghosh, A. Shekhter, F. Jerzembeck, N. Kikugawa, D. A. Sokolov, M. Brando, A. P. Mackenzie, C. W. Hicks, and B. J. Ramshaw, Thermodynamic evidence for a two-component superconducting order parameter in Sr_2RuO_4, Nat. Phys. **17**, 199 (2021).